

The nature of the laning transition in two dimensions

This article has been downloaded from IOPscience. Please scroll down to see the full text article.

2012 J. Phys.: Condens. Matter 24 464114

(<http://iopscience.iop.org/0953-8984/24/46/464114>)

View [the table of contents for this issue](#), or go to the [journal homepage](#) for more

Download details:

IP Address: 134.99.64.185

The article was downloaded on 02/11/2012 at 08:42

Please note that [terms and conditions apply](#).

The nature of the laning transition in two dimensions

T Glanz and H Löwen

Institut für Theoretische Physik II: Weiche Materie, Heinrich-Heine-Universität Düsseldorf, D-40225 Düsseldorf, Germany

E-mail: glanz@thphy.uni-duesseldorf.de

Received 19 March 2012, in final form 21 May 2012

Published 31 October 2012

Online at stacks.iop.org/JPhysCM/24/464114

Abstract

If a binary colloidal mixture is oppositely driven by an external field, a transition towards a laned state occurs at sufficiently large drives, where particles driven alike form elongated structures ('lanes') characterized by a large correlation length ξ along the drive. Here we perform extensive Brownian dynamics computer simulations on a two-dimensional equimolar binary Yukawa system driven by a constant force that acts oppositely on the two species. We systematically address finite-size effects on lane formation by exploring large systems up to 262 144 particles under various boundary conditions. It is found that the correlation length ξ along the field depends exponentially on the driving force (or Peclet number). Conversely, in a finite system, ξ reaches a fraction of the system size at a driving force which is logarithmic in the system size, implying massive finite-size corrections. For a fixed finite drive, ξ does not diverge in the thermodynamic limit. Therefore, though laning has a signature as a sharp transition in a finite system, it is a smooth crossover in the thermodynamic limit.

(Some figures may appear in colour only in the online journal)

1. Introduction

In equilibrium, there is a fundamental difference between a sharp phase transition which exhibits a jump in a certain derivative of the free energy with respect to a thermodynamic variable [1] and a continuous crossover where no such discontinuity exists in the thermodynamic limit. This is much less clear for nonequilibrium phase transitions since a free energy does not exist in general there. Here, in many situations, an order parameter can still be defined in the steady state and hysteresis behaviour typically serves as a criterion to discriminate between discontinuous and continuous behaviour. Another approach is to focus on the divergence of a correlation length in order to reveal a critical point in nonequilibrium [2].

While it is by now well understood how the order of an equilibrium phase transition is controllable by the interparticle interactions [3–5], the question of which key parameters determine the existence and order of nonequilibrium phase transitions is much less understood due to the multitude of parameters characterizing the nature of the dynamics [6–9].

Lane formation in a binary mixture of Brownian particles which are driven by a constant external force depending on the particle species [10] represents a prototype

of a nonequilibrium transition in a continuous (i.e. off-lattice) system [11]. Previous Brownian dynamics computer simulations have strongly supported the scenario that for increasing driving force the system undergoes a transition from a mixed steady state towards a steady state where macroscopic lanes are formed. Such a laning transition has been found in Brownian dynamics computer simulations of models for oppositely driven repulsive mixtures [10, 12–16] in two and three spatial dimensions. The laning behaviour was later quantitatively confirmed both in complex plasmas [17] and in oppositely charged colloidal mixtures driven by an electric field [18, 19]. Moreover, lane formation occurs in driven granular matter [20, 21] as well as in active matter composed of autonomously moving agents such as pedestrians [22, 23], social insects [24], bacteria and cells [25, 26], and artificial colloidal microswimmers [27].

In two spatial dimensions, it was found from relatively small system sizes [10] that a suitable order parameter which detects laning exhibits a significant hysteresis—if the driving force is increased and subsequently decreased—which signals a discontinuous nonequilibrium phase transition. This is in contrast to three dimensions, where the analogous model does not exhibit hysteretic behaviour [28–30].

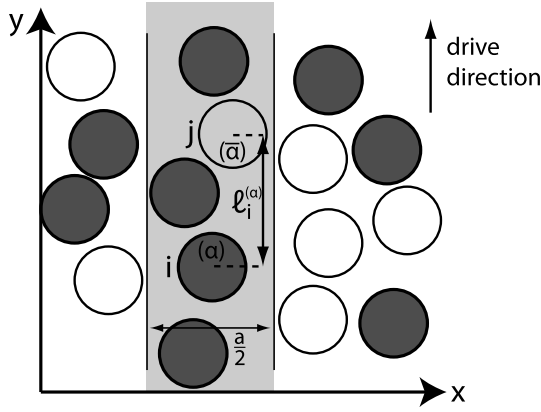


Figure 1. Sketched calculation of ℓ_i . We consider a stripe around a particle of type α and measure the distance to the closest complementary particle of type $\bar{\alpha}$ within this stripe.

Here, we revisit the question whether the transition towards lane formation is discontinuous or has a smooth crossover in a two-dimensional system by using a large-scale Brownian dynamics computer simulation for a repulsive Yukawa mixture. The mixture is driven by a constant external force F which acts oppositely on the two species. We study systematically finite-size effects by exploring large systems up to 262 114 particles under various boundary conditions. In particular we consider the behaviour of a correlation length ξ along the drive which characterizes the length of the lanes. Therefore, though laning has a signature as a sharp transition in a finite system, as found in previous simulations [10], it is a smooth crossover in the thermodynamic limit. We further explore the influence of the boundary conditions on the laning behaviour by studying both periodic and shifted boundary conditions. As typical, for phase transition in nonequilibrium [31–33], a strong influence of the boundary conditions on the structuring in the steady state is found, which, however, does not affect the exponential dependency of ξ on F .

This paper is organized as follows: in section 2 we propose the model and the simulation technique. Results are discussed in section 3. Finally, section 4 contains conclusions and a discussion of possible future work.

2. The model

In our Brownian dynamics computer simulations [34], we consider an equimolar binary mixture of N particles interacting via the screened Coulomb potential

$$V(r) = V_0 \frac{\exp(-\kappa r)}{r} \quad (1)$$

in two spatial dimensions (following [10, 35]), where r denotes the central distance between two particles. Here V_0 measures an interaction amplitude and κ is the inverse screening length. A Yukawa pair potential is an established model for the interaction between charged colloidal suspensions [36, 37], also in confinement between two charged plates [38]. All particles interact via the same potential irrespective of their species. The system is simulated in the canonical ensemble at fixed particle number N ($N/2$

particles for each species), area A and temperature T . The mean interparticle distance a defined as $a = \sqrt{A/N}$ serves as unit of length, and the thermal energy $k_B T$ is a suitable energy scale. Anticipating that our qualitative results do not depend on interaction and thermodynamic details, we fixed $\kappa a = 6$ and $V_0 a / k_B T = 0.3$ throughout all of our simulations.

The external field $\vec{F}^{(\alpha)}$ acting along the y -direction depends, however, on the particles species α ($\alpha = 1, 2$):

$$\vec{F}^{(\alpha)} = (-1)^\alpha F \vec{e}_y, \quad (2)$$

such that the particles are driven in opposite directions. It is convenient to introduce the dimensionless Peclet number Pe to characterize the strength of the drive as

$$Pe = \frac{Fa}{k_B T}. \quad (3)$$

We vary the Peclet number in the range from zero up to 160.

The simulation is performed in a rectangular box of dimensions L_x and L_y such that the total area of the system is $A = L_x L_y$. There are periodic boundary conditions in the x -direction perpendicular to the drive. The boundary conditions in the field direction are either periodic (as considered in most of our simulations) or shifted. Due to the drive, the box length L_y in drive direction is expected to be more crucial than L_x , therefore we choose $L_y = 4L_x$ in most of our simulations. The initial configuration at time $t = 0$ is taken from an equilibrated drive-free simulation. Time-dependent trajectories of the particles are calculated using a finite-time step method with a diagonal diffusion tensor [34] characterized by a short-time diffusion constant D_0 . The latter serves to define a Brownian timescale $\tau_B = a^2 / D_0$. After an initial relaxation period t_0 , the system runs into a steady state. We take steady-state statistics within a time window of about $100\tau_B$. The finite time-step used in the simulation was $\Delta t = 10^{-4}\tau_B$.

Let us now define a correlation length characterizing the typical length of the lanes. Let $\{\vec{r}_i^\alpha\} = \{(x_i^\alpha, y_i^\alpha)\}$ be a particle configuration, where $\alpha = 1, 2$ is the species index and the index $i = 1, \dots, N/2$ labels the particles of the same species. To measure the extent of laning we associate with each particle i of species α a length scale ℓ_i^α , as obtained from its anisotropic local surrounding. The idea is to consider only opposite particles which are within a stripe of width $\frac{a}{2}$, as expressed by an index set $\mathcal{I}_i^{(\alpha)} = \{j\}$ of indices j which all fulfil the condition

$$|x_i^\alpha - x_j^{\bar{\alpha}}| \leq \frac{a}{2}. \quad (4)$$

Here we defined the species index $\bar{\alpha}$, which is complementary to α , by

$$\bar{\alpha} = \begin{cases} 1 & \text{for } \alpha = 2 \\ 2 & \text{for } \alpha = 1. \end{cases} \quad (5)$$

Under this condition we look for the next oppositely driven particle with the smallest distance from the i th particle, as sketched in figure 1. This distance characterizes the length of

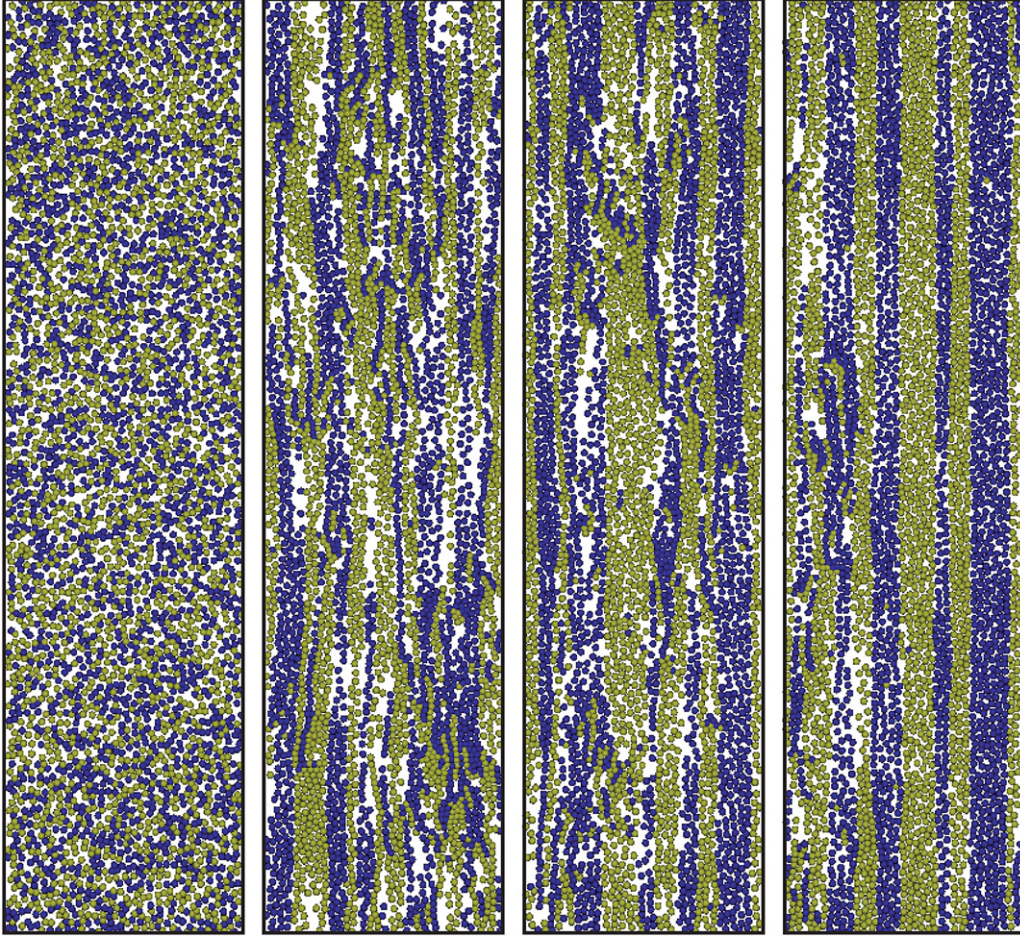


Figure 2. Typical snapshots of a computer simulation with $N = 4096$ particles for the relaxation into the laned steady state at $Pe = 115$ after a time of (a) $0\tau_B$ (initial mixed configuration), (b) $2\tau_B$, (c) $8\tau_B$ and (d) $20\tau_B$. Particles of different species are differently coloured. The white regions contain no particles at all.

a lane in the y -direction, hence

$$\ell_i^\alpha = \min_{j \in \mathcal{I}_i^\alpha} |y_i^\alpha - y_j^\alpha|. \quad (6)$$

In the case there is no oppositely charged particle in the observed lane, we set $\ell_i^\alpha = L_y$ corresponding to a system-spanning lane. We construct a histogram of ℓ_i^α when averaged over all particles, species and steady-state configurations, and therefore obtain a normalized distribution function $P(\ell)$ of the distances. Finally, we define the first moment of this distribution as a system correlation length ξ , namely

$$\xi = \langle \ell_i^\alpha \rangle \equiv \langle \ell \rangle = \int_0^\infty d\ell \ell P(\ell) \quad (7)$$

with $\langle \dots \rangle$ denoting an average over all particles and steady-state configurations [39].

3. Results

For the relaxation into the steady state after applying the external drive, typical simulation snapshots for $N = 4096$ particles are shown in figure 2 for a high Peclet number

$Pe = 115$, where a strong degree of laning is developing. The system moves to a completely laned state after about $20\tau_B$. One should note, however, that for larger times the lanes are not static but constantly change and intermix.

In figure 3, we show snapshots in the steady state for different drives. One clearly sees the tendency to form longer and more pronounced lanes as the Peclet number Pe increases.

It is important to get a clear idea about the duration of the relaxation process in order not to obscure steady-state averages with transient initial effects. We point out that the relaxation time t_0 needed to get into the steady state depends on the driving strength. We have monitored the relaxation of the correlation length ξ in order to estimate t_0 . For $N = 65\,536$ particles, an example is presented in figure 4(a), plotted logarithmically over a broad time window for two different Peclet numbers $Pe = 60$ and 120 .

The saturation of ξ to its steady-state value occurs after about $t_0 = 2\tau_B$ for $Pe = 60$ and after about $t_0 = 100\tau_B$ for $Pe = 150$. Basically, ξ increases with time, indicating the steady built-up of lanes. Before reaching the steady-state limit, there are significant fluctuations. This estimate for t_0 is consistent with monitoring the potential energy during

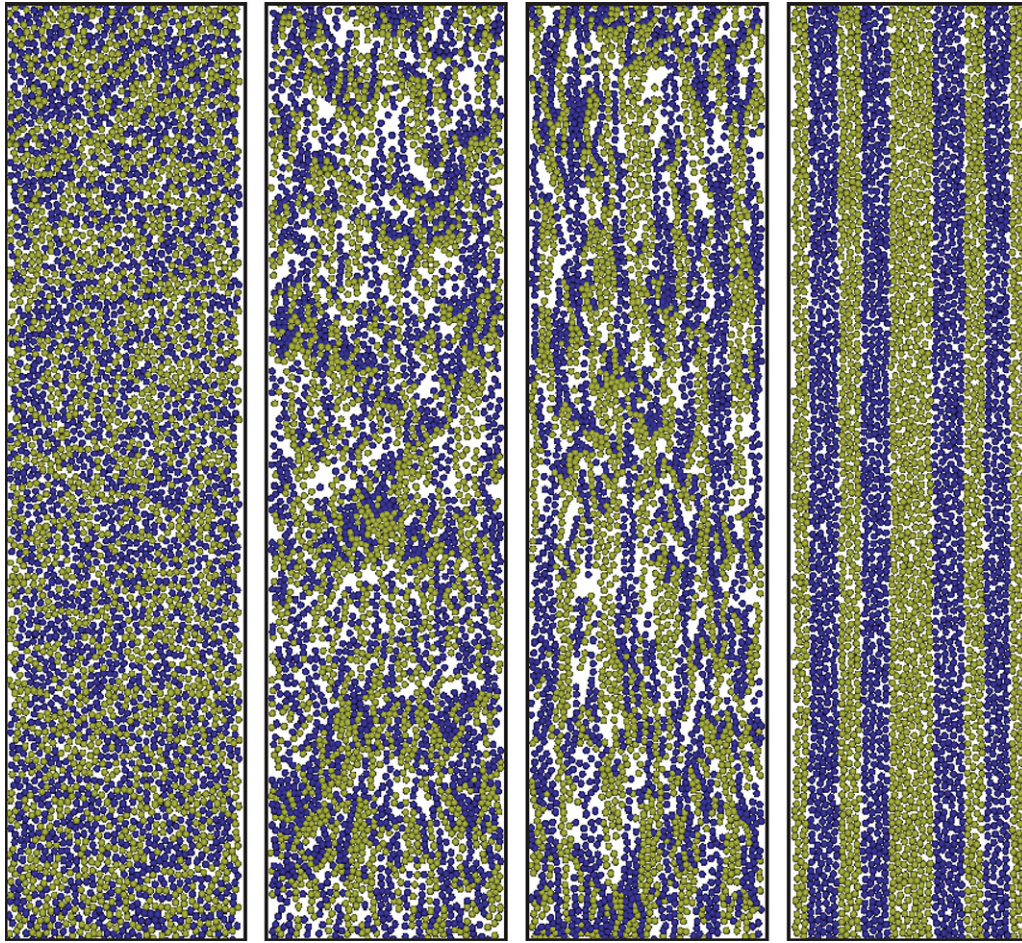


Figure 3. Typical snapshots of a computer simulation with $N = 4096$ particles in the steady state for (a) $Pe = 0$ (mixture in equilibrium) (b) $Pe = 40$, (c) $Pe = 80$ and (d) $Pe = 160$. Particles of different species are differently coloured.

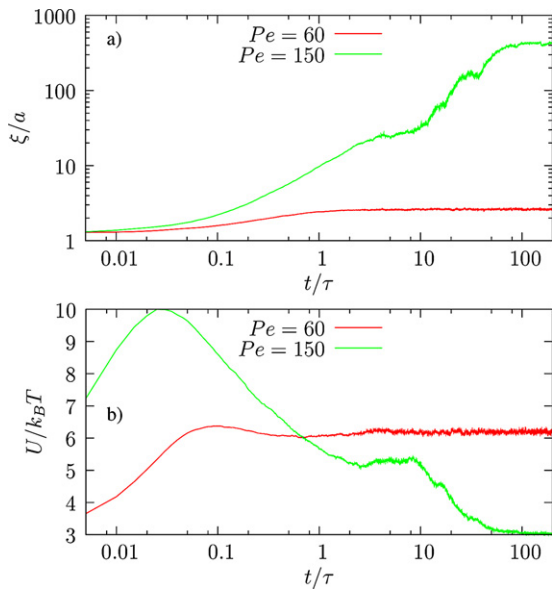


Figure 4. Temporal development of (a) the correlation length ξ and (b) total potential energy per particle $\frac{U}{k_B T}$ during relaxation for two Peclet numbers $Pe = 10$ and $Pe = 150$ with $N = 65\,536$.

relaxation, which is conveniently chosen to characterize the relaxation processes [40]. In fact, the relaxation of the total potential energy U per particle is shown over the same time window in figure 4(b) for the same two Peclet numbers $Pe = 60$ and 120 . In general, the potential energy increases initially and then decreases towards its steady-state limit. This has to do with the fact that, after getting started from a mixed configuration at time $t = 0$, the opposite drive increases the separation between particles of different species which increases U while subsequent laning causes a decrease of these energetically costly collisions. If the relaxation time t_0 is estimated from the potential energy saturation, the data are close to that gained from the saturation of the correlation length ξ , compare figures 4(a) and (b)¹. Finally, one should also bear in mind that the relaxation time depends slightly on the system size.

Figure 5 shows the correlation length ξ versus driving strength Pe for different particle numbers N . Periodic boundary conditions were used. Small sizes give the same correlation length for low Peclet number but start to deviate from the data of larger system sizes when the correlation length becomes comparable to the system size L_y in the drive

¹ Another marker for the relaxation process is the mechanical pressure.

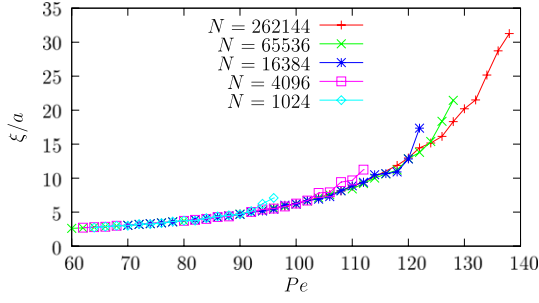


Figure 5. Correlation length ξ in the steady state versus external drive Pe for different particle numbers N .

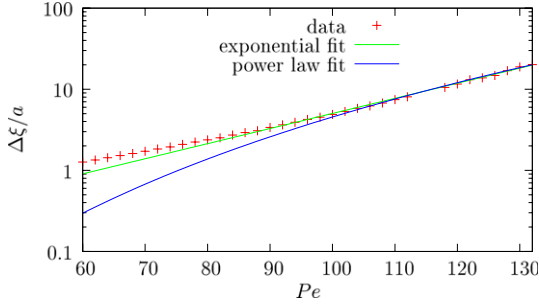


Figure 6. Semi-logarithmic plot of the exponential fit and the power-law fit for the correlation length data $\Delta\xi(Pe)/a$.

direction. Using this plot as a reference one can conclude that the data of the largest system size are reliable up to about $Pe = 132$ and define uniquely a dimensionless function $\xi(Pe)/a$. We have tried to approximate this function by various fits. In particular, a good description was achieved by an exponential fit

$$\xi(Pe) = \xi(0) + A \left(\exp\left(\frac{Pe}{Pe_0}\right) - 1 \right) \quad (8)$$

with two fit parameters $A = 0.069$ and $Pe_0 = 23.3$ and $\xi(0) = 1.35a$ determined from the equilibrium simulations. As an alternate fit, the following power law was used

$$\xi(Pe) = \xi(0) + BPe^\gamma \quad (9)$$

again with two fitting parameters $B = 9.18 \times 10^{-11}$ and an exponent $\gamma = 5.35$. As becomes evident from a semi-logarithmic plot of $\Delta\xi(Pe) = (\xi(Pe) - \xi(0))$, shown in figure 6, the exponential fit is better than the power-law fit over the range of Peclet numbers between 60 and 132. Figure 6 in fact reveals a linear dependence of the data over a full decade, thus confirming the exponential fit of equation (8). Hence we conclude that based on our simulation data the correlation length depends exponentially on the drive such that for large drives:

$$\xi(Pe) \propto \exp\left(\frac{Pe}{Pe_0}\right). \quad (10)$$

As a further check of finite system size effects, we have scaled the full data for the correlation length by the finite box length L_y . The results for all system sizes explored are shown in figure 7. The data for ξ/L_y are obviously bounded

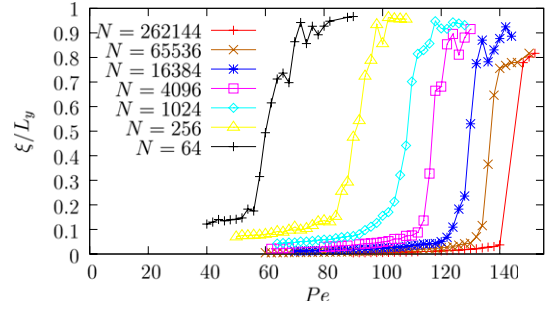


Figure 7. Plot of ξ/L_y versus driving strength Pe for different system sizes N .

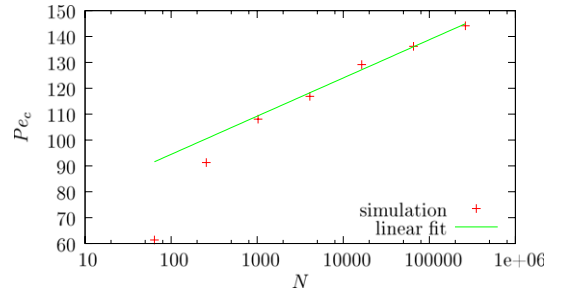


Figure 8. Critical Peclet number Pe_c characterizing the inflection points versus particle number N on a semi-logarithmic representation. A linear fit to the data is also shown.

between 0 and 1. For a given system size the correlation length ξ quickly switches in a relative small range of Peclet numbers from small values to system-size comparable ones. In this range, for each fixed system size N , we have fitted the following hyperbolic Fermi–Dirac-like approximation to the data

$$\xi(Pe)/L_y = b + \frac{c}{1 + d \exp(Pe/f)} \quad (11)$$

where b, c, d and f are fit parameters. The inflection point of this fit gives a good measure to the point where the correlation length becomes comparable with the system size and defines a system-size dependent critical Peclet number $Pe_c(N)$. This critical Peclet number is shown on a semi-logarithmic plot in figure 8. Over more than two decades of system sizes, a linear behaviour reveals that the system size corrections are logarithmic, i.e.

$$Pe_c(N) \propto \ln(L_y) \propto \ln(N). \quad (12)$$

This is consistent with equation (8): if one sets ξ equal to a fraction of L_y , the resulting critical Peclet number is logarithmic in L_y . From the slope of the linear fit shown in figure 8, one gets to leading order $Pe_c(N) = 14 \ln(L_y/a)$, where the prefactor 14 is smaller but of the same order of magnitude as the parameter $Pe_0 = 23.3$ found in the exponential fit in equation (8). The difference in the two prefactors is consistent with the fact that the correlation length is larger in a finite system (as induced by the periodic boundary conditions).

As a more general remark, logarithmic size corrections are dramatic, they also destroy long-range positional order in

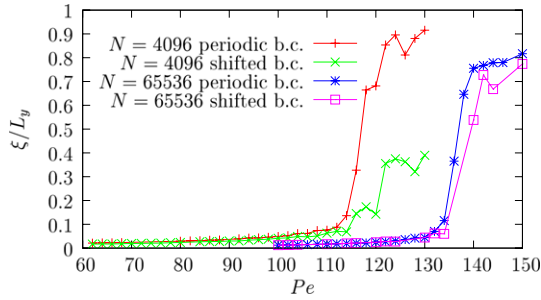


Figure 9. Plot of $\frac{\xi(Pe)}{L_y}$ from two types of simulations with $N = 65\,536$ particles using either periodic or shifted boundary conditions.

two-dimensional equilibrium crystallization [41] and occur in other circumstances [42, 43]. For a review see [44]. As the most basic conclusion we therefore state that, for finite drives, system-spanning lanes only occur for infinite-large systems, i.e. in the thermodynamic limit.

We finally address the stability of our results with respect to other boundary conditions in the drive direction. We have introduced a shift by $\pm 0.5a$ in the x -direction if a particle leaves the simulation box. This is unfavourable for lanes extended in the y -direction. Our large-scale simulations show that shifted boundary conditions affect the critical Pelet number Pe_c but not the actual exponential behaviour obtained when ξ is much smaller than L_y . In other words, the exponential fit (8) is independent of the boundary conditions and the logarithmic law (12) persists. The actual proportionality prefactor in (12), however, depends slightly on the boundary conditions. This is documented by simulation data for two particle numbers $N = 4096$ and $N = 65\,536$ shown in figure 9. While the boundary conditions change the critical Pelet number by about 10% for small system sizes ($N = 4096$), the deviations drop to about 3% for $N = 65\,536$ if the inflection point criterion is used to determine Pe_c . The boundary conditions, however, do not affect the data in the low- ξ wing needed to extract the exponential fit of equation (8).

4. Conclusions

In conclusion, we have systematically explored finite-size effects for the laning transition. Our main conclusion is that perfect laning with system-spanning lanes occurs only at infinitely high driving forces. Lane formation is therefore a continuous crossover, but the length of the lanes depends exponentially on the drive. In previous experiments [17, 45] the lanes observed were pretty short, much smaller than the system size at finite drive. This is at least qualitatively compatible with our findings, although there is a caveat since the experiments of [17, 4] were conducted in three dimensions. In previous simulations, the system size was too small to clearly see the finite-size corrections, which are logarithmic in the system size. However, the onset of the laning transition is consistent with previous work if finite lanes composed of 3–10 particles are considered.

We finally point out that there is a formal similarity of laning to the glass transition, which is also generally understood to be a nonequilibrium phenomenon. The drive leading to glass formation is thermodynamic and achieved by cooling the system. For strong glass formers [46–50], the characteristic timescale τ_α (corresponding to our correlation length) diverges exponentially with the inverse temperature $1/T$ (corresponding to the Pelet number of this study), as described by an Arrhenius law $\tau_\alpha \propto \exp(T_0/T)$, where T_0 is a material-dependent scale. Traditionally one states that a system is glassy when the timescale τ_α exceeds an experimentally observable time window. In our situation, this translates to the fact that the correlation length becomes of the order of the observable system size. Of course, further work is needed to explore this possible formal analogy between glass formation and laning in more detail.

Future work should address the following open questions: first, it would be interesting to study the nature of the laning in three spatial dimensions. Then similar two lanes spanning the system in drive direction can merge without crossing an oppositely driven lane. Therefore, one can speculate that the order of the laning is different in 3D. Second, in zero-temperature models (similar to that proposed in [11]) laning can emerge as a second-order transition. This is, however, different to our model where the temperature is finite. Third, the influence of hydrodynamic interactions on laning should be studied more. The latter can be accessed either by diffusion tensors [28] or by more advanced simulation schemes such as multi-particle collision dynamics [51, 45]. Fourth, there is a need to study laning on theoretical grounds by a microscopic nonequilibrium theory based on the Smoluchowski equation, similar to what has been proposed for external shear fields [52]. This would extend previous approaches where a phenomenological current term was needed as an input [13, 53]. A first approach was recently proposed in [54]. Finally, there are a few further questions which should be explored in future studies including: (i) the emergence and formation of lanes in the initial relaxation towards the steady state, (ii) the typical life-time of a finite-extended lane in the steady state, (iii) the distribution of the (horizontal) thicknesses of the lanes during the relaxation process, (iv) a full phenomenological construction of finite-size scaling and (v) a simulation of the particle currents in order to compare them with phenomenological assumptions [13, 53].

Acknowledgments

We thank A Ivlev, M Kohl and J Chakrabarti for helpful discussions. This work was supported by the DFG within SFB TR6 (project C3).

References

- [1] Callen H 1960 *Thermodynamics* (New York: Wiley)
- [2] Schmittmann B and Zia R 1998 *Phys. Rep.* **301** 45
- [3] Löwen H 1994 *Phys. Rep.* **237** 249
- [4] Lekkerkerker H 1997 *Physica A* **244** 227

- [5] Poon W 1998 *Curr. Opin. Colloid Interface* **3** 593
- [6] Ramaswamy S 2010 *Ann. Rev. Condens. Matter Phys.* **1** 323
- [7] Shrivastav G P, Banerjee V and Puri S 2010 *Phase Transit.* **83** 140
- [8] Löwen H 2001 *J. Phys.: Condens. Matter* **13** R415
- [9] Rüdiger S, Nicola E M, Casademunt J and Kramer L 2007 *Phys. Rep.* **447** 73
- [10] Dzubiella J, Hoffmann G P and Löwen H 2002 *Phys. Rev. E* **65** 021402
- [11] Corte L, Chaikin P, Gollub J and Pine D 2008 *Nature Phys.* **4** 420
- [12] Netz R 2003 *Europhys. Lett.* **63** 616
- [13] Chakrabarti J, Dzubiella J and Löwen H 2003 *Europhys. Lett.* **61** 415
- [14] Löwen H and Dzubiella J 2003 *Faraday Discuss.* **123** 99
- [15] Delhomme J 2005 *Phys. Rev. E* **71** 016705
- [16] Pandey R, Gettrust J, Seyfarth R and Cueva-Parra L 2003 *Int. J. Mod. Phys. C* **14** 955
- [17] Sütterlin K R *et al* 2009 *Phys. Rev. Lett.* **102** 085003
- [18] Leunissen M *et al* 2005 *Nature* **437** 235
- [19] Vissers T *et al* 2011 *Soft Matter* **7** 2352
- [20] Ehrhardt G C M A, Stephenson A and Reis P M 2005 *Phys. Rev. E* **71** 041301
- [21] Ciamarra M P, Coniglio A and Nicodemi M 2005 *Phys. Rev. Lett.* **94** 188001
- [22] Jiang R, Helbing D, Shukla P and Wu Q 2006 *Physica A* **368** 567
- [23] Kölbl R and Helbing D 2003 *New J. Phys.* **5** 48
- [24] Chowdhury D, Nishinari K and Schadschneider A 2004 *Phase Transit.* **77** 601
- [25] Wensink H H and Löwen H 2012 *J. Phys.: Condens. Matter* **24** 464130
- [26] Yamao M, Naoki H and Ishii S 2011 *PLoS One* **6** e27950
- [27] McCandlish S R, Baskaran A and Hagan M F 2012 *Soft Matter* **8** 2527
- [28] Rex M and Löwen H 2008 *Eur. Phys. J. E* **26** 143
- [29] Rex M and Löwen H 2007 *Phys. Rev. E* **75** 051402
- [30] Löwen H 2010 *Soft Matter* **6** 3133
- [31] Krug J 1991 *Phys. Rev. Lett.* **67** 1882
- [32] Frey E and Kroy K 2005 *Ann. Phys., Lpz.* **14** 20
- [33] Nagy M, Daruka I and Vicsek T 2007 *Physica A* **373** 445
- [34] Allen M and Tildesley D 1989 *Computer Simulation of Liquids* (New York: Clarendon)
- [35] Reichhardt C and Reichhardt C J O 2006 *Phys. Rev. E* **74** 011403
- [36] Löwen H and Allahyarov E 1998 *J. Phys.: Condens. Matter* **10** 4147
- [37] Hansen J-P and Löwen H 2000 *Annu. Rev. Phys. Chem.* **51** 209
- [38] Allahyarov E, D'Amico I and Löwen H 1999 *Phys. Rev. E* **60** 3199
- [39] Wysocki A and Löwen H 2009 *Phys. Rev. E* **79** 041408
- [40] Assoud L *et al* 2009 *Phys. Rev. Lett.* **102** 238301
- [41] Fröhlich J and Pfister C 1981 *Comm. Math. Phys.* **81** 277
- [42] Affleck I and Qin S 1999 *J. Phys. A: Math. Gen.* **32** 7815
- [43] Janke W 1997 *Phys. Rev. B* **55** 3580
- [44] Binder K 1997 *Rep. Prog. Phys.* **60** 487
- [45] Wysocki A and Löwen H 2011 *J. Phys.: Condens. Matter* **23** 284117
- [46] Alba-Simionesco C, Caillaux A, Alegría A and Tarjus G 2004 *Europhys. Lett.* **68** 58
- [47] Paluch M, Gapinski J, Patkowski A and Fischer E 2001 *J. Chem. Phys.* **114** 8048
- [48] Richert R 2002 *J. Phys.: Condens. Matter* **14** R703
- [49] Debenedetti P G and Stillinger F H 2001 *Nature* **410** 259
- [50] Ivlev A V, Löwen H, Morfill G E and Royall C P 2012 *Complex Plasmas and Colloidal Dispersions: Particle-Resolved Studies of Classical Liquids and Solids* (Singapore: World Scientific)
- [51] Gompper G, Ihle T, Kroll D M and Winkler R G 2009 *Advanced Computer Simulation Approaches for Soft Matter Sciences III (Advances in Polymer Science vol 221)* ed C Holm and K Kremer (Berlin: Springer) pp 1–87
- [52] Bławdziewicz J and Szamel G 1993 *Phys. Rev. E* **48** 4632
- [53] Chakrabarti J, Dzubiella J and Löwen H 2004 *Phys. Rev. E* **70** 012401
- [54] Kohl M *et al* 2012 *J. Phys.: Condens. Matter* **24** 464115